American Mineralogist, Volume 85, pages 1512–1515, 2000

Rietveld refinement of okayamalite, $Ca_2SiB_2O_7$: Structural evidence for the B/Si ordered distribution

G. GIULI,* L. BINDI, AND P. BONAZZI†

Dipartimento di Scienze della Terra, Via La Pira 4, I-50121 Firenze, Italy

ABSTRACT

The structure of okayamalite from Arendal, Norway, was refined using the Rietveld method, with Co$K\alpha$ powder X-ray diffraction data (R_F = 3.69%). Okayamalite exhibits a melilite-type structure, space group $P\bar{4}2_1m$, with cell edges a = 7.1248(2), c = 4.8177(2) Å. Si and B are ordered on the T1 and T2 sites respectively, in agreement with the refined tetrahedral distances (<T1-O> = 1.657 Å and <T2-O>= 1.498 Å). In comparison with the other melilite-type compounds, the cation population in okayamalite leads to the minimum structural misfit between tetrahedral and square-antiprism layers.

INTRODUCTION

Subsequent to the pioneering work of Bauer (1962) on Al-B diadochy in the synthetic compound $Ca_2SiB_2O_7$, Tarney (1973) obtained boron melilite by heating datolite and concluded that Si is probably ordered on the T1 site on the basis of the theoretical powder X-ray diffraction (XRD) pattern. Further investigation by means of infrared spectroscopy (Kimata 1978) gave additional evidence that Si is ordered on the T1 site. Boron melilite (okayamalite) was found in nature as milky white aggregates in skarn samples at the Fuka Mine, Okayama district, Japan (Matsubara et al. 1998). Okayamalite was recently found in a skarn rock from the Arendal district, Sørlandet, Norway (Olmi et al. 2000). The sample from Arendal occurs as a fine intergrowth of crystalline okayamalite and amorphous silica on the scale of ~100 Å (Olmi et al. 2000). To date, no crystal structure refinement has been reported for okayamalite or its synthetic analog. In this paper, we report the structure obtained for the sample from Arendal.

EXPERIMENTAL METHODS

Several grains were separated by hand picking and were finely ground in an agate mortar. Due to the scarcity of material, the sample was prepared as a thin layer on a single-crystal Si sample-holder by allowing the powder to settle gently in acetone. Step-scan powder XRD data were recorded with an automated Philips diffractometer equipped with diffracted-beam Soller slits, 1° divergence slits, 0.1 mm receiving slits, and a graphite-diffracted beam monochromator. The long-fine focus Co X-ray tube was operated at 40 kV, 20 mA. The spectrum was recorded in the 2θ range 10–140°, with a 0.02° step and 9 s counting time. Si powder (NBS 640a) was used as external standard to check the accuracy of the refined 2θ zero shift.

* Present address: Dipartimento di Scienze della Terra, Unità INFM dell'Università di Camerino, Via Gentile III da Varano, I-62032 Camerino (MC), Italy.
† E-mail: pbcry@steno.geo.unifi.it

RIETVELD STRUCTURE REFINEMENT

The structure was refined with the program GSAS (Larsen and Von Dreele 1994). The peak shape was modeled with a pseudo-Voigt function; the FWHM was refined as a function of 2θ, taking into account both Gaussian and Lorentian broadening. The intensity cut-off for the calculation of the profile-step intensity was 0.1% of the peak maximum.

The refinement was carried out in the space group $P\bar{4}2_1m$. Starting atomic coordinates were those of the synthetic compound $Ba_2MgSi_2O_7$ (Shimizu et al. 1995), with initial values for isotropic temperature factors (U_{iso}) arbitrarily chosen as 0.04 Å^2 for Ca, 0.02 Å^2 for Si and B, 0.025 Å^2 for O. The atom sites were designated fully occupied. Si was assigned to the T1 site and B to the T2 site. The background was modeled as a 12-term polynomial function. Cell parameters, scale factor, and the background polynomial functions were free variables during refinement. Parameters were added to the refinement in the following order: 2θ zero-shift, peak-shape, peak-asymmetry, sample-displacement, atomic coordinates, and isotropic temperature factors. During the refinement of the atomic coordinates, a soft constraint was applied to the <B-O> distance (1.48 Å) with the constraint weight being progressively lowered until the coordinates were allowed to vary without constraints. We assumed final convergence to be reached when the parameter shifts were <1% of their respective e.s.d. values. Refinement of preferred orientation according to the March model (Dollase 1986) did not improve the fit. In fact, the refined coefficient was always very close to 1.0, indicating there was no preferential orientation; thus it was neglected in the subsequent refinements. Trials performed using different models with B disordered over the T1 and T2 sites yielded unsatisfactory results in terms of profile fitting (Table 1). In particular, by constraining the Si/B distribution to be disordered, the refinement diverged with negative isotropic temperature factors. Moreover, further trials were done starting from differently disordered Si-B distributions and refining tetrahedral occupancies without constraints. The resulting distributions, however, were always

found to be fully ordered. In Table 1, the relevant data of the final refinement are reported together with the *R* values obtained for the other two models with the same structural parameters but different tetrahedral occupancies.

The observed, calculated, and difference powder XRD patterns are shown in Figure 1. Detailed examination of the observed pattern shows the absence of diffraction peaks belonging to any crystalline phase other than okayamalite. As noted by Olmi et al. (2000), a broad feature can be observed approximately centered at $2\theta \approx 25.9°$ (d ≈ 4.0 Å), which is due to amorphous silica minutely intergrown with okayamalite. Atomic coordinates are listed in Table 2 along with isotropic displacement parameters (U_{iso}), whereas interatomic distances are listed in Table 3.

TABLE 1. Relevant data of the refinement

	okayamalite		
space group	$P\bar{4}2_1m$		
a	7.1248(2) Å		
c	4.8177(2) Å		
V	244.56(1) Å^3		
	(a)	(b)	(c)
Rwp	11.41%	35.78%	20.62%
Rp	8.58%	24.70%	15.58%
R_F^2	5.87%	35.04%	15.93%
R_F	3.69%	21.04%	8.98%

Note: *R* indexes are reported for the following configurations respectively: (a) $[Si]_{T1} + 2[B]_{T2}$; (b) $[B]_{T1} + 2[B_{0.5}Si_{0.5}]_{T2}$; (c) $[B_{0.5}Si_{0.5}]_{T1} + 2[B_{0.75}Si_{0.25}]_{T2}$.

TABLE 2. Fractional atomic coordinates and isotropic displacement parameters, with their e.s.d. values (in parentheses)

Site	Position	*x/a*	*y/b*	*z/c*	U_{iso} (Å^2)
X(Ca)	4(e)	0.3384(2)	½ – x	0.5080(4)	0.020(1)
T1(Si)	2(a)	0	0	0	0.019(1)
T2(B)	4(e)	0.1408(4)	½ – x	0.9470(9)	0.013(2)
O1	2(c)	½	0	0.1460(2)	0.013(2)
O2	4(e)	0.1424(5)	½ – x	0.2517(7)	0.013(1)
O3	8(f)	0.0782(4)	0.1777(4)	0.8105(7)	0.013(1)

TABLE 3. Interatomic distances (Å), angles (°), and distortion indexes (λ and σ^2) with their e.s.d. values in parentheses

X-O1	2.386(5)
X-O2	2.329(5)
X-O2 ×2	2.460(4)
X-O3 ×2	2.361(4)
X-O3 ×2	2.566(4)
T1-O3 ×4	1.657(1)
λ_{T1}	1.0021
σ^2_{T1}	8.03
T2-O1	1.488(1)
T2-O2	1.468(1)
T2-O3 ×2	1.518(1)
λ_{T2}	1.0067
σ^2_{T2}	25.68
T1-O3-T2	120.73(2)
T2-O1-T2	144.95(2)

Note: The mean quadratic elongation (λ) and the angle variance (σ^2) were computed according to Robinson et al. (1971).

CRYSTAL CHEMICAL REMARKS

The structure of okayamalite is topologically identical to that of the other melilite-type compounds (Shimizu et al. 1995, and references therein). Only minor variations, related to the chemical composition, affect bond distances and angles in okayamalite (Table 3). The structure consists of layers of corner-sharing [$T1O_4$] and [$T2_2O_7$] groups, resulting in an arrangement of tetrahedra with large pentagonal interstices where projected along the c axis. Stacking of adjacent layers results in channels that are occupied by Ca cations. The latter are coordinated by eight oxygen atoms at the vertices of a distorted square antiprism.

As expected, Si was found to occupy the larger T1 tetrahedron, whereas B fills the T2 tetrahedron to form B_2O_7 groups. The <T1-O> distance (1.657 Å), although rather long for a pure Si-O bond (Liebau 1985), is close to that observed (1.67 Å) by Bartram (1969) in synthetic $Y_2SiBe_2O_7$, the only melilite-type compound with T1 completely filled by Si. Those unusually long T1-O distances can be related to charge balance consideration: due to the entry of a tetravalent cation in T1, the O3 oxygen is here the most overbonded anion in the structure (2.13 u.v. on the basis of the empirical method of Brown and Altermatt 1985). Thus, a decrease of the T1-O3 bond distance would further enhance the O3 overbonding. The <T2-O> bond length of 1.498 Å can be compared with those found in other borosilicates containing B_2O_7 groups: 1.483 and 1.490 Å in taramellite (Mazzi and Rossi 1980), 1.474 Å in danburite (Phillips et al. 1974), and 1.487 and 1.495 Å in hellandite (Oberti et al. 1999).

On the whole, okayamalite shows the smallest mean size of the tetrahedral layer among the melilite-type structures. As pointed out by Seifert et al. (1987), geometrical restrictions exist in terms of the size of the tetrahedral cations with respect to the size of the interlayer X cations (Ca, Sr, Ba, Y, etc.). The greater the size of tetrahedra with respect to X-polyhedra, the bigger the structural strain and the consequent deformation of the sheet of tetrahedra. Therefore, due to the small size of T1 and T2 tetrahedra, crystal-chemical behavior of okayamalite approaches that of melilite-type structures where cations larger than Ca (Sr or Ba) occupy the interlayer interstices. This interpretation is made evident by plotting some structural parameters against the T/X ratio, with T/X= [(<T1-O>+2<T2-O>)/3<X-O>]. In Figure 2, the T1-O3-T2 angles are plotted against T/X for several melilite-type compounds. Okayamalite shows a rather high value for the T1-O3-T2 angle (120.73°): as the relative size of the tetrahedral layer increases, the bending between pairs of tetrahedra increases to reduce the structural misfit with the layer made up by X cations. A particularly low value, in fact, is observed in the structure of $Ca_2ZnGe_2O_7$ (Armbruster et al. 1990) where the structural misfit is maximum due to the large size of Ge that enters T2. As the T/X ratio increases, the T2 tetrahedron becomes more irregular, as made evident from the values of angular distortion σ^2_{T2} (Fig. 3). The T2 tetrahedron, in fact, shares three edges with three XO_8 polyhedra; as is expected on the basis of Pauling's rules, the shared edges are shorter than the unshared ones. As the size of the T2 cation increases, a preferential lengthening of the unshared edges occurs and consequently the tetrahedral distortion becomes greater. On the contrary, any substitution of larger cations (e.g.,

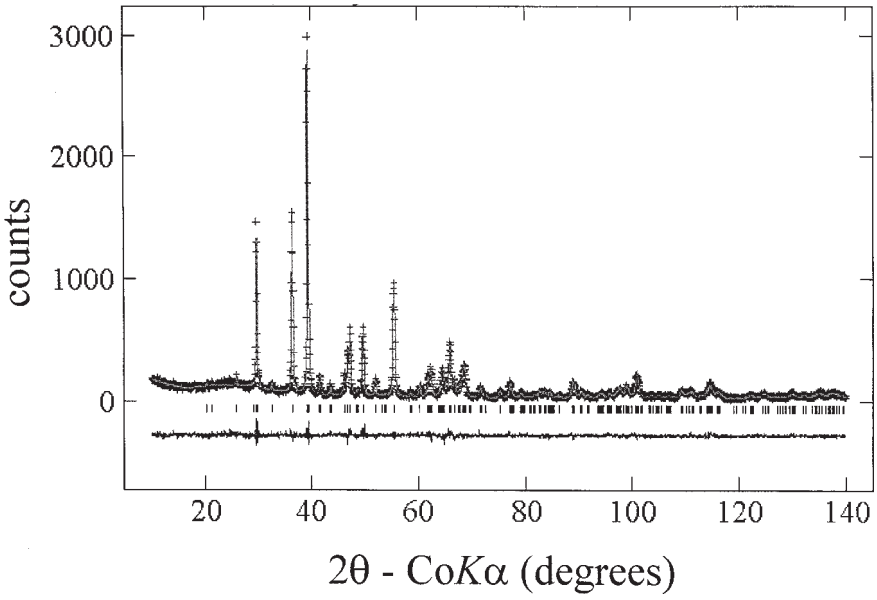

FIGURE 1. Experimental (crosses), theoretical (solid line), and difference (solid line at the bottom) powder XRD patterns. Reflection positions are marked by vertical bars.

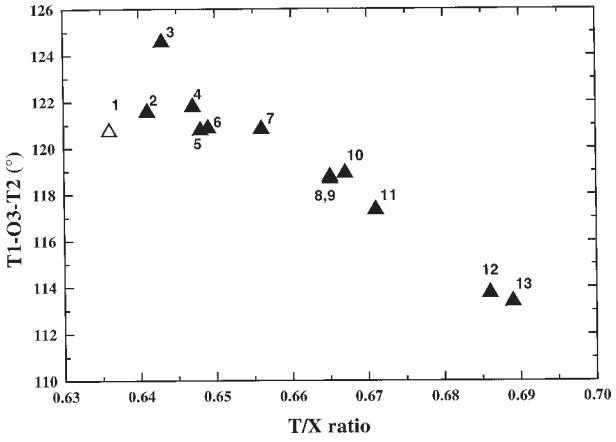

FIGURE 2. Values of the T1-O3-T2 angle plotted against the T/X ratio (see text). Empty symbol (1) refers to okayamalite. Black symbols (2–13) refer to literature data. (2) $Sr_2Al_2SiO_7$ Kimata 1984; (3) $Ba_2MgSi_2O_7$ Shimizu et al. 1995; (4) $Sr_2MgSi_2O_7$ Kimata 1983a; (5) $Ca_2BeSi_2O_7$ Kimata and Ohashi 1982; (6) $CaNaAlSi_2O_7$ Louisnathan 1970; (7) $Sr_2MnSi_2O_7$ Kimata 1985; (8) $Ca_2Al_2SiO_7$ Kimata and Ii 1982; (9) $Ca_2CoSi_2O_7$ Kimata 1983b; (10) $Ca_2MgSi_2O_7$ Kimata and Ii 1981; (11) $Ca_2ZnSi_2O_7$ Louisnathan 1969; (12) $Y_2SiBe_2O_7$ Bartram 1969; (13) $Ca_2ZnGe_2O_7$ Armbruster et al. 1990.

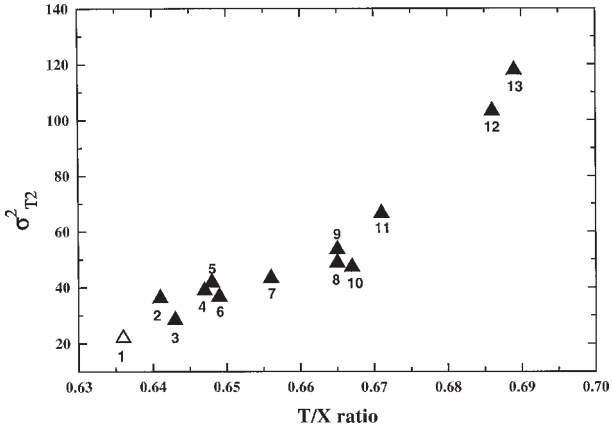

FIGURE 3. Values of angular distortion σ^2 calculated according to Robinson et al. (1971) plotted against the T/X ratio (see text). Empty symbol (1) refers to okayamalite. Black symbols (2–13) refer to the same data as in Figure 2.

Sr, Ba) for Ca leads to a decrease of the distortion of the T2 tetrahedron. A similar trend is shown by the mean quadratic elongation λ_{T2}. Therefore, among the known melilite-type structures, okayamalite, due to its chemical composition, has the best atomic arrangement to minimize the intrinsic structural strain between the tetrahedral and the XO_8 layer. This accounts for the lack of structural modulation on the basis of TEM investigations (Olmi et al. 2000).

ACKNOWLEDGMENTS

Critical and careful reviews by two official referees and by Associate Editor Gilberto Artioli were greatly appreciated. Many thanks are also due to Silvio Menchetti for his helpful suggestions. Joanne Krueger checked the readibility of the manuscript. This work was funded by M.U.R.S.T., "cofinanziamento 1999," project "Transformations, reactions, ordering in minerals."

REFERENCES CITED

Armbruster, T., Röthlisberger, F., and Seifert, F. (1990) Layer topology, stacking variation, and site distortion in melilite-related compounds in the system CaO-ZnO-GeO_2-SiO_2. American Mineralogist, 75, 847–858.

Bartram, S.F. (1969) Crystal structure of $Y_2SiBe_2O_7$. Acta Crystallographica, B25, 791–795.

Bauer, H. (1962) Uber Diadochie zweischen Aluminium und Bor in Gehlenit. Neues Jahrbuch für Mineralogie Monatshefte, 1962, 127–140.
Brown J.D. and Altermatt D. (1985) Bond-valence parameters obtained from a systematic analysis of the inorganic crystal structure database. Acta Crystallographica, B41, 244–247.
Dollase, W.A. (1986). Correction of intensities for preferred orientation in powder diffractometry: application of the March model. Journal of Applied Crystallography, 19, 267–272.
Kimata, M. (1978) Boron behaviour in the thermal decomposition of datolite. Neues Jahrbuch für Mineralogie Monatshefte, 1978, 58–70.
———(1980) Crystal chemistry of Ca-melilites on X-ray diffraction and infrared absorption properties. Neues Jahrbuch für Mineralogie Abhandlungen, 139, 43–58.
———(1983a) The structural properties of synthetic Sr-åkermanite, $Sr_2MgSi_2O_7$. Zeitschrift für Kristallographie, 163, 295–304.
———(1983b) The crystal structure and stability of Co-åkermanite, $Ca_2CoSi_2O_7$, compared with the mineralogical behaviour of Mg cation. Neues Jahrbuch für Mineralogie Abhandlungen, 146, 221–241.
———(1984) The structural properties of synthetic Sr-gehlenite, $Sr_2Al_2SiO_7$. Zeitschrift für Kristallographie, 167, 103–116.
———(1985) The structural properties and mineralogical significance of synthetic $Sr_2MnSi_2O_7$ melilite with 4-coordinated manganese. Neues Jahrbuch für Mineralogie Monatshefte, 85–96.
Kimata, M. and Ii, N. (1981) The crystal structure of synthetic åkermanite, $Ca_2MgSi_2O_7$. Neues Jahrbuch für Mineralogie Monatshefte, 1981, 1–10.
———(1982) The structural property of synthetic gehlenite, $Ca_2Al_2SiO_7$. Neues Jahrbuch für Mineralogie Abhandlungen, 144, 254–267.
Kimata, M. and Ohashi, H. (1982) The crystal structure of synthetic gugiaite, $Ca_2BeSi_2O_7$. Neues Jahrbuch für Mineralogie Abhandlungen, 143, 210–222.
Larsen, A.C. and Von Dreele, R.B. (1994) GSAS. General Structure Analysis System. LANSCE, MS-H805, Los Alamos, New Mexico.
Liebau, F. (1985) Structural chemistry of silicates. Springer-Verlag Ed., Berlin.
Louisnathan, S.J. (1969) Refinement of the crystal structure of hardystonite, $Ca_2ZnSi_2O_7$. Zeitschrift für Kristallographie, 130, 427–437.
———(1970) The crystal structure of synthetic soda melilite, $CaNaAlSi_2O_7$. Zeitschrift für Kristallographie, 131, 314–321.
Matsubara, S., Miyawaki, R., Kato, A., Yokoyama, K., and Okamoto, A. (1998) Okayamalite, $Ca_2B_2SiO_7$, a new mineral, boron analogue of gehlenite. Mineralogical Magazine, 62, 703–706.
Mazzi, F. and Rossi, G. (1980) The crystal structure of taramellite. American Mineralogist, 65, 123–128.
Oberti, R., Ottolini, L. Camara, F., and Della Ventura, G. (1999) Crystal structure of non-metamict Th-rich hellandite-(Ce) from Latium (Italy) and crystal chemistry of hellandite-group minerals. American Mineralogist 84, 913–921.
Olmi, F., Viti, C., Bindi, L., Bonazzi, P., Menchetti, S. (2000) Second occurrence of okayamalite, $Ca_2SiB_2O_7$: chemical and TEM characterization. American Mineralogist, 85, 1508–1511.
Phillips, M.W., Gibbs, G.V., and Ribbe, P.H. (1974) The crystal structure of damburite: a comparison with anorthite, albite and reedmergnerite. American Mineralogist 59, 79–85.
Robinson, K., Gibbs, G.V., and Ribbe, P.H. (1971) Quadratic elongation: a quantitative measure of distortion in coordination polyhedra. Science, 172, 567–570.
Seifert, F., Czank, M., Simons, B., and Schmahl, W. (1987) A commensurate-incommensurate phase transition in iron-bearing åkermanite. Physics and Chemistry of Minerals, 14, 26–35.
Shimizu, M., Kimata, M., and Iida, I. (1995) Crystal structure of $Ba_2MgSi_2O_7$: the longest tetrahedral Mg-O distance. Neues Jahrbuch für Mineralogie Monatshefte, 1995, 39–47.
Tarney, J., Nicol, A.W., and Marriner, G.F. (1973) The thermal transformation of datolite, $CaBSiO_4(OH)$, to boron-melilite. Mineralogical Magazine, 39, 158–175.

MANUSCRIPT RECEIVED NOVEMBER 23, 1999
MANUSCRIPT ACCEPTED MAY 26, 2000
PAPER HANDLED BY GILBERTO ARTIOLI